

Control Laws for UAV Formation Flying

Martina Chiaramonti* and Giovanni Mengali†

Department of Aerospace Engineering, University of Pisa, I-56122 Pisa, Italy

Abstract

Unmanned aircraft formation control has recently become an important and growing research field. The interest in this research area is due to the wide quantity of applications, either civil or military, as, for example, survey missions in adverse environment. Most of UAV formation control systems developed until now make use of two-dimensional formation models, while in this paper we propose a control law, based on a nonlinear dynamic inversion approach, whose aim is to maintain a desired three-dimensional geometry formation.

1 Nomenclature

C_L	=	lift coefficient
C_D	=	drag coefficient
C_Y	=	side force coefficient
C_l	=	roll coefficient
C_m	=	pitch coefficient
C_n	=	yaw coefficient
D	=	drag
F_x	=	body force along x axis
F_y	=	body force along y axis
F_z	=	body force along z axis
J_i	=	i -th moment of inertia (kg m^2)
k_i	=	i -th gain
L	=	lift (N)
\bar{L}	=	rolling moment (Nm)
M	=	pitching moment (Nm)
N	=	yawing moment (Nm)
T	=	thrust (N)
Y	=	side-Force (N)
V	=	velocity (m/s)
b	=	wingspan (m)
\bar{c}	=	mean aerodynamic chord (m)
g	=	gravitational acceleration (m/s^2)
m	=	aircraft mass (kg)
p	=	roll rate (rad/s)
q	=	pitch rate (rad/s)
\bar{q}	=	dynamic pressure ($\text{kg}/(\text{m s}^2)$)
r	=	yaw rate (rad/s)
x	=	position along longitudinal x axis (m)
y	=	position along lateral y axis (m)

h = position along vertical h axis (m)

Acronyms

NLDI = Nonlinear Dynamic Inversion
UAV = Unmanned Aerial Vehicles

Greek letters

α = angle of attack (rad)
 β = angle of sideslip (rad)
 δ_a = aileron deflection (rad)
 δ_e = elevator deflection (rad)
 δ_r = rudder deflection (rad)
 ν = new input
 ϕ = roll angle (rad)
 ψ = pitch angle (rad)
 ρ = air density (kg/m^3)
 θ = yaw angle (rad)

Subscripts

des = desired
 f = follower
 x = projection along x axis
 y = projection along y axis
 h = projection along z axis

2 Introduction

Aircraft formation control has become an active research area both for the challenge it offers from the control system viewpoint and for the innumerable advantages it presents in different aerospace applications. In particular, the popularity of Uninhabited Aerial Vehicles (UAV) has substantially increased in recent years and, indeed, UAV flight formation is already playing a major role in most military operation.

In a manner similar to migratory birds, aircraft in a formation may experience a substantial drag reduction using the vortex upwash created by the leading aircraft, with potential fuel reduction and significant benefits for both military and commercial employments. However, the enormous potential of autonomous vehicles, especially low cost, small size UAV is far from being fully realized.

For example, future employments will involve the terrestrial monitoring in hostile environments, with applications involving not only the military sphere (weapon detections, enemy surveillance), but also the civil field^[1] (rescue, fire location, etc.). In these cases

*PhD student, Email: martina.chiaramonti@ing.unipi.it

†Associate Professor, Email: g.mengali@ing.unipi.it

the strength of a formation flight based mission lies, on one side, in a wider coverable surface and, on the other side, on the fact that it removes any risk of life losses. The UAV cluster utilization is desirable not only for its logistic and technical qualities, but also for the economic characteristic of such a solution. In fact, an important economical aspect is the cheapness in manufacturing a few number of equal, small aircrafts when compared to a unique bigger aircraft. Furthermore, as regularly demonstrated by migrating birds, aircraft in a formation can experience a drag reduction by close flight by exploiting the wakes generated by the other aircrafts. This may translate in a substantial fuel consumption reduction, an important feature especially for long duration missions. Finally, autonomous formation flight systems are widely investigated due to their close connection to the aerial refuelling problem.^[2,3]

In order to guarantee the advantages related to the formation flight, it is usually required to maintain a prescribed formation geometry. Accordingly, autonomous formation flight represents a challenging task both from the viewpoint of flight dynamics and that of flight control. Most of the existing literature is concerned with the problem of aircraft formation control^[4,5,6,7,8] and/or aerodynamic interference modelling,^[9,10,11] while a fixed formation structure is assumed. Although various structures have been proposed,^[4,5,6,7,8,12,13] here we assume a formation based on a leader-follower structure. The first aircraft in the formation is designated as the leader, with the other aircraft treated as followers. While the leader aircraft maintains a given trajectory, the followers refer their position to a prescribed formation geometry, that is, track a fixed relative distance from the neighboring aircraft. The advantage of such a structure lies in its simplicity and, therefore, it is widely employed in control and management of multiple vehicle formations.

The aim of this work is to establish a control architecture which is able to maintain the prescribed formation geometry. Such a goal is achieved using a control system architecture constituted by two loops. The outer one uses the nonlinear dynamics inversion theory to obtain the commands required for the geometry maintenance, while the inner loop guarantees that the desired command tracking is achieved. A detailed example demonstrates the effectiveness of the proposed methodology.

3 Formation Modeling

Assuming that the leader is following a desired trajectory, our goal is to control the generic follower flight path starting from the knowledge of that of the leader and of the formation geometry.

4 Aircraft Equations of Motion

The nonlinear aircraft mathematical model is described by the following set of nonlinear differential equations characterizing the flight dynamics of a rigid aircraft flying in a stationary atmosphere over a flat and non-rotating Earth.^[14]

$$\begin{aligned}
\dot{V} &= \frac{1}{m} (F_x \cos \alpha \cos \beta + F_y \sin \beta + F_z \sin \alpha \sin \beta) \\
\dot{\alpha} &= \frac{1}{m V \cos \beta} (-F_x \sin \alpha + F_z \cos \alpha) + q + \\
&\quad - (p \cos \alpha + r \sin \alpha) \tan \beta \\
\dot{\beta} &= (-F_x \cos \alpha \sin \beta + F_y \cos \beta - F_z \sin \alpha \sin \beta) / (m V) \\
&\quad + p \sin \alpha - r \cos \alpha \\
\dot{x} &= V [\sin \beta (\sin \phi \sin \theta \cos \psi - \cos \phi \sin \psi) \\
&\quad + \cos \beta \sin \alpha (\cos \phi \sin \theta \cos \psi + \sin \phi \sin \psi) \\
&\quad + \cos \beta \cos \alpha \cos \theta \cos \psi] \\
\dot{y} &= V [\sin \beta (\sin \phi \sin \theta \sin \psi + \cos \phi \cos \psi) \\
&\quad + \cos \beta \sin \alpha (\cos \phi \sin \theta \sin \psi - \sin \phi \cos \psi) \\
&\quad + \cos \beta \cos \alpha \cos \theta \sin \psi] \\
\dot{h} &= V (\cos \beta \cos \alpha \sin \theta - \sin \beta \sin \phi \cos \theta + \\
&\quad - \cos \beta \sin \alpha \cos \phi \cos \theta)
\end{aligned} \tag{1}$$

$$\begin{aligned}
\dot{\theta} &= q \cos \phi - r \sin \phi \\
\dot{\psi} &= q \sin \phi \sec \theta + r \cos \phi \sec \theta \\
\dot{\phi} &= p + q \sin \phi \tan \theta + r \cos \phi \tan \theta
\end{aligned}$$

$$\begin{aligned}
\dot{p} &= (c_1 r + c_2 p) q + c_3 L + c_4 N \\
\dot{q} &= c_5 p r - c_6 (p^2 - r^2) + c_7 M \\
\dot{r} &= (c_8 p - c_2 r) q + c_4 L + c_9 N
\end{aligned}$$

The c_i coefficients are defined in appendix A, while F_x , F_y and F_z are the body forces, that is:

$$\begin{aligned}
F_x &= T - D \cos \alpha + L \sin \alpha - mg \sin \theta \\
F_y &= Y + mg \cos \theta \sin \phi \\
F_z &= -D \sin \alpha - L \cos \alpha + mg \cos \theta \cos \phi
\end{aligned} \tag{2}$$

For convenience we define also the force component F_x^* as

$$F_x^* \triangleq F_x - T \tag{3}$$

5 Control System

The control system has been arranged as shown in Fig. 1. It comprises an outer loop, which implements a Nonlinear Dynamic Inversion (NLDI)-based controller, and a faster inner loop, which allows the actuation of commands through the control surfaces. For each aircraft (A/C) in the formation the vector \mathbf{y} of measured outputs is fed back to the NLDI control system, which also receives, as an input information, the vector of reference trajectory from the formation leader. The aim

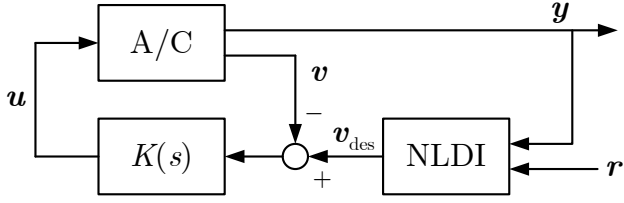


Fig. 1: Control system architecture.

of the NLDI is to compare the actual aircraft position with the reference one and to generate the commands necessary to attain a tracking of the desired trajectory. The outputs of the the NLDI block are in form of a vector \mathbf{v} of “virtual” inputs, which is processed by the inner loop (constituted by a linear controller $K(s)$ and by an aircraft linearized model) to generate the actual vector \mathbf{u} of aircraft command inputs. More precisely, the trajectory tracking is obtained by acting on throttle, elevator and aileron commands.

5.1 Outer Loop

The outer loop is constituted by a NLDI-based controller. The aim of NLDI approach is to reduce algebraically a nonlinear system into a linear one. In essence, the fundamental ideas can be summarized as follows. Assume that a generic nonlinear dynamics system is described in the form:

$$\dot{\mathbf{x}} = \mathbf{f}(\mathbf{x}, \mathbf{v}) \quad (4)$$

$$\mathbf{y} = \mathbf{g}(\mathbf{x}) \quad (5)$$

where \mathbf{x} is the state vector, \mathbf{y} is the measurable output vector and \mathbf{v} is the input vector. If one derives the output vector w.r.t. the time up to a suitable order n , the input is recovered explicitly as:^[15]

$$\mathbf{y}^{(n)} = \mathbf{F} + \mathbf{G}\mathbf{v} \quad (6)$$

Therefore, provided that the \mathbf{G} matrix is invertible, it is possible to accomplish the following algebraic transformation:

$$\mathbf{v} = \mathbf{G}^{-1}[\mathbf{v} - \mathbf{F}] \quad (7)$$

This allows one to obtain a linear dynamics system:

$$\mathbf{y}^{(n)} = \mathbf{v} \quad (8)$$

The latter can be controlled with classic techniques, using a suitable form for the \mathbf{v} expression.

Our specific problem is featured by the generic aircraft position given in an Earth local vertical frame, or

$$\mathbf{y} = [x_f \quad y_f \quad h_f]^T \quad (9)$$

where subscript f refers to the follower aircraft, while the vector of “virtual” inputs is constituted by the pitch-rate $\dot{\theta}$, the thrust command T and the lateral force F_y :

$$\mathbf{v} = [\dot{\theta} \quad T \quad F_y]^T \quad (10)$$

According to NLDI theory, the output equations are derived w.r.t. the time until Eq. (6) is recovered. The result is

$$\begin{aligned} m\ddot{x}_f &= -Vm(\cos\beta\cos\alpha\sin\phi - \sin\beta\cos^2\phi\cos\psi\cos\theta \\ &\quad + \cos\beta\sin\alpha\sin\phi\cos\psi\cos\phi\cos\theta + \sin\theta\cos\psi \\ &\quad + \cos\theta\cos\psi\sin\beta)r + \cos\theta\cos\psi F_x^* + \\ &\quad + (\sin\phi\sin\psi + \cos\phi\sin\theta\cos\psi)F_z + \\ &\quad - Vm[\sin\beta\cos\psi\cos\theta\cos\phi\sin\phi + \\ &\quad - \cos\beta\cos\psi\sin\theta\cos\alpha\cos\phi + \\ &\quad - \cos\beta\cos\psi\cos\theta\sin\alpha\cos\phi^2]q + \\ &\quad + Vm[\sin\beta\cos\psi\cos\theta\sin\phi + \\ &\quad + \cos\beta\cos\psi\sin\theta\cos\alpha + \\ &\quad + \cos\beta\cos\psi\cos\theta\sin\alpha\cos\phi]\dot{\theta} \\ &\quad + \cos\theta\cos\psi T + \\ &\quad + (\sin\phi\sin\theta\cos\psi - \cos\phi\sin\psi)F_y \\ m\ddot{y}_f &= Vm\sin\psi(\cos\theta\sin\beta - \cos\beta\cos\alpha\sin\phi\sin\theta \\ &\quad + \cos\beta\sin\alpha\sin\phi\cos\phi\cos\theta - \sin\beta\cos^2\phi\cos\theta)r \\ &\quad + \cos\theta\sin\psi F_x^* \\ &\quad + (\cos\phi\sin\theta\sin\psi - \sin\phi\cos\psi)F_z \\ &\quad + Vm\sin\psi\cos\phi[\cos\beta\sin\theta\cos\alpha + \\ &\quad - \sin\beta\cos\theta\sin\phi - \cos\beta\cos\theta\sin\alpha\cos\phi]q + \\ &\quad + Vm\sin\psi[\cos\beta\cos\theta\sin\alpha\cos\phi + \\ &\quad + \sin\beta\cos\theta\sin\phi - \cos\beta\sin\theta\cos\alpha]\dot{\theta} \\ &\quad + (\cos\phi\cos\psi + \sin\phi\sin\theta\sin\psi)F_y \\ &\quad + \cos\theta\sin\psi T \\ m\ddot{h}_f &= Vm(\cos\beta\sin\alpha\sin\phi\cos\phi\sin\theta + \sin\theta\sin\beta \\ &\quad + \cos\beta\sin\phi\cos\theta\cos\alpha - \sin\beta\cos^2\phi\sin\theta)r \\ &\quad + \sin\theta F_x^* - \cos\phi\cos\theta F_z \\ &\quad + Vm\cos\phi[-\cos\beta\cos\theta\cos\alpha - \sin\beta\sin\theta\sin\phi \\ &\quad - \cos\beta\sin\theta\sin\alpha\cos\phi]q \\ &\quad + Vm[\cos\beta\cos\theta\cos\alpha \\ &\quad + \sin\beta\sin\theta\sin\phi + \cos\beta\sin\theta\sin\alpha\cos\phi]\dot{\theta} \\ &\quad + \sin\theta T - \sin\phi\cos\theta F_y \end{aligned}$$

The relationships between the output derivatives and the virtual inputs have been inverted to obtain the algebraic transformation which describes the system according to Eq. (8). The resulting linear system is controlled by solving a pole assignment problem for each channel as follow:

$$\begin{aligned} \nu_1 &= \ddot{x}_{des} - k_{x_d}(\dot{x} - \dot{x}_{des}) - k_{x_p}(x - x_{des}) \\ \nu_2 &= \ddot{y}_{des} - k_{y_d}(\dot{y} - \dot{y}_{des}) - k_{y_p}(y - y_{des}) \\ \nu_3 &= \ddot{h}_{des} - k_{h_d}(\dot{h} - \dot{h}_{des}) - k_{h_p}(h - h_{des}) \end{aligned} \quad (11)$$

Note that each channel behaves like a pure second order system whose dynamics can be chosen by the designer through the proportional and derivative gains k_{x_p} , k_{x_d} ,

k_{y_p} , k_{y_d} , k_{h_p} and k_{h_d} . As a result of the preceding procedure, the virtual inputs have been obtained as a function of the reference (that is “desired”) position and its derivative. The explicit expressions for the virtual inputs are given in Appendix B.

5.2 Inner Loop

The inner loop controller is composed by both a lateral-directional and a longitudinal channel, whose purposes are to track the desired inputs. As far as the thrust is concerned, in a first approximation the engine dynamics has been neglected, and the desired command has been directly introduced into the aircraft dynamics equations.

5.2.1 Longitudinal Controller

The longitudinal inner loop controller is a linear controller that tracks the desired angular rate $\dot{\theta}$ using the elevator deflection command.

5.2.2 Lateral-Directional Controller

The lateral-directional inner loop controller is a linear controller that tracks the desired lateral force F_y using the ailerons deflection command. Also, the stability of the roll rate channel is augmented with a classic yaw damper.

5.3 Formation Flight Simulation

The procedure described above has been implemented in a Simulink-based simulation program for formation constituted by two identical UAV. The geometric, inertial and aerodynamic data of both aircraft have been taken by the database available at West Virginia University, where these vehicles have been designed, built and tested.^[16] The aircraft geometric, inertial and aerodynamic data of the aircraft model have been summarized in Tab. 1–3.

\bar{c}	=	0.7649 m	b	=	1.9622 m
S	=	1.3682 m ²	m	=	20.6384 kg
J_x	=	1.61 kg m ²	J_y	=	7.51 kg m ²
J_z	=	7.18 kg m ²	J_{xz}	=	-0.59 kg m ²

Tab. 1: Aircraft geometric and inertial data

The simulation results are shown in Figs. 2–7.

C_{D_0}	=	0.08
C_{D_α}	=	0.508 rad ⁻¹
C_{D_q}	=	0
$C_{D_{\delta_e}}$	=	-0.0339 rad ⁻¹
C_{L_0}	=	-0.049
C_{L_α}	=	3.258 rad ⁻¹
C_{L_q}	=	0
$C_{L_{\delta_e}}$	=	0.189 rad ⁻¹
C_{m_0}	=	0.0226
C_{m_α}	=	-0.4738 rad ⁻¹
C_{m_q}	=	-3.449 rad ⁻¹
$C_{m_{\delta_e}}$	=	-0.3644 rad ⁻¹

Tab. 2: Longitudinal aerodynamic derivatives

C_{Y_0}	=	0
C_{Y_β}	=	0.2725 rad ⁻¹
C_{Y_p}	=	1.2151 rad ⁻¹
C_{Y_r}	=	-1.1618 rad ⁻¹
$C_{Y_{\delta_a}}$	=	0.1836 rad ⁻¹
$C_{Y_{\delta_r}}$	=	-0.4592 rad ⁻¹
C_{l_0}	=	0
C_{l_β}	=	-0.0380 rad ⁻¹
C_{l_p}	=	-0.2134 rad ⁻¹
C_{l_r}	=	0.1147 rad ⁻¹
$C_{l_{\delta_a}}$	=	-0.0559 rad ⁻¹
$C_{l_{\delta_r}}$	=	0.0141 rad ⁻¹
C_{n_0}	=	0
C_{m_β}	=	0.0361 rad ⁻¹
C_{n_p}	=	-0.1513 rad ⁻¹
C_{n_r}	=	-0.1958 rad ⁻¹
$C_{n_{\delta_a}}$	=	-0.0358 rad ⁻¹
$C_{n_{\delta_r}}$	=	-0.0555 rad ⁻¹

Tab. 3: Lateral-directional aerodynamic derivatives

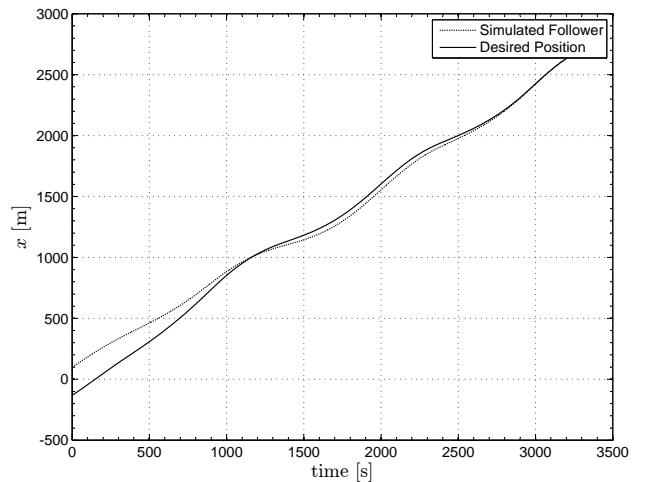


Fig. 2: Comparison between desired and simulated x -position.

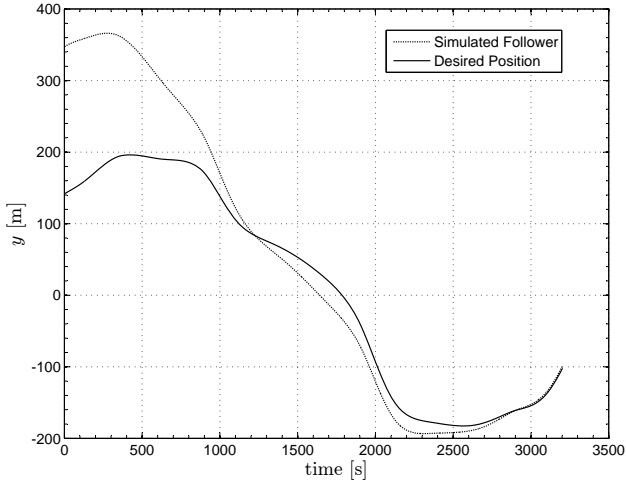


Fig. 3: Comparison between desired and simulated y -position.

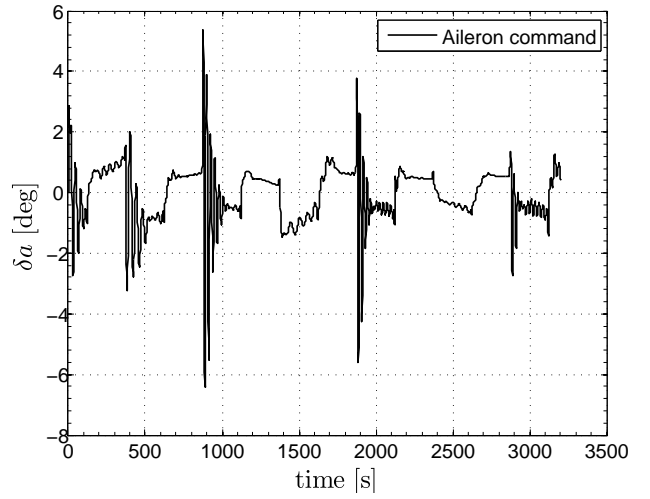


Fig. 5: Time history of aileron deflection to track the desired trajectory.

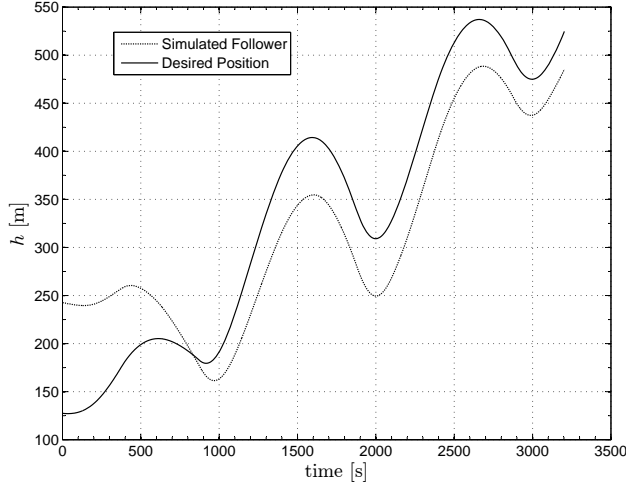


Fig. 4: Comparison between desired and simulated vertical position.

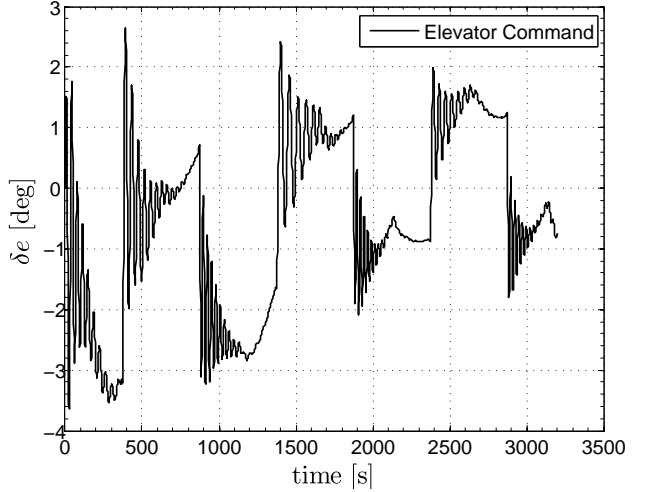


Fig. 6: Time history of elevator deflection to track the desired trajectory.

6 Conclusions

This paper, aimed to demonstrating a successful application of NLDI to the design of UAV formation guidance laws, introduces a innovative concept consisting in the use of such a design methodology for a three-dimensional aircraft formation control. The control system is constituted by two loops; the outer one makes use of a NLDI approach to obtain the command history, while the inner one realizes the tracking of the commands with classic linear methods. The simulation results show the effectiveness of the proposed methodology.

Appendix A

The inertial coefficients are defined as follows. Define:

$$\Gamma \triangleq J_x J_y - J_{xz}^2$$

then

$$c_1 = [(J_x - J_z)J_z - J_{xz}^2]/\Gamma$$

$$c_2 = [(J_x - J_y + J_z)J_{xz}]/\Gamma$$

$$c_3 = J_z/\Gamma$$

$$c_4 = J_{xz}/\Gamma$$

$$c_5 = (J_z - J_x)/J_y$$

$$c_6 = J_{xz}/J_y$$

$$c_7 = 1/J_y$$

$$c_8 = [J_x(J_x - J_y) + J_{xz}^2]/\Gamma$$

$$c_9 = J_x/\Gamma$$

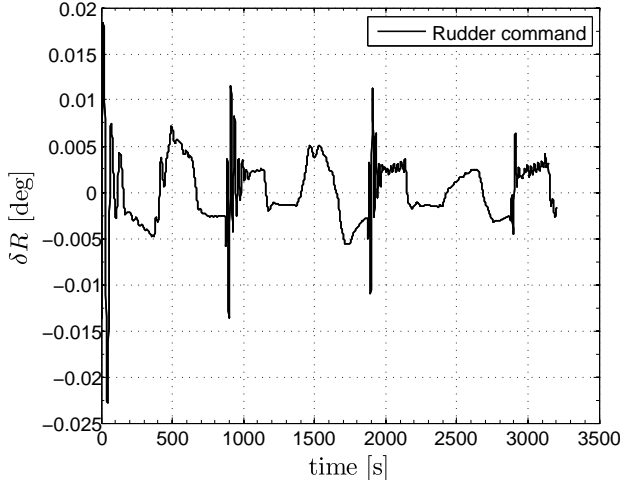


Fig. 7: Time history of rudder deflection to track the desired trajectory.

Appendix B

In this appendix we give the explicit relationships for the virtual inputs, according to Eq. (7).

$$T_{\text{des}} = \frac{1}{\cos \beta \cos \alpha \cos \phi} \left(-\sin \beta \sin \phi F_z + \right. \\
-\sin \alpha \cos \phi \cos \beta F_z + \\
-\cos \phi \cos \beta \cos \alpha F_x^* + \\
+m \sin \theta \cos \phi \cos \beta \cos \alpha \nu_3 + \\
+m \sin \beta \sin \phi \sin \theta \cos \psi \cos \phi \nu_1 + \\
+m \cos \psi \cos \theta \cos \phi \cos \beta \cos \alpha \nu_1 + \\
+m \cos \theta \sin \psi \cos \phi \cos \beta \cos \alpha \nu_2 + \\
-m \sin \alpha \cos^2 \phi \cos \theta \cos \beta \nu_3 + \\
+m \sin \alpha \cos^2 \phi \sin \theta \sin \psi \cos \beta \nu_2 + \\
+m \sin \alpha \cos^2 \phi \sin \theta \cos \psi \cos \beta \nu_1 + \\
+m \sin \alpha \sin \psi \sin \phi \cos \phi \cos \beta \nu_1 + \\
-m \sin \beta \sin \psi \cos^2 \phi \nu_1 + \\
+m \sin \beta \sin \psi \nu_1 - m \sin \beta \cos \psi \nu_2 + \\
+m \sin \beta \sin \phi \sin \theta \sin \psi \cos \phi \nu_2 + \\
+m \sin \beta \cos^2 \phi \cos \psi \nu_2 + \\
-m \sin \alpha \sin \phi \cos \psi \cos \phi \cos \beta \nu_2 + \\
\left. -m \sin \beta \sin \phi \cos \theta \cos \phi \nu_3 \right)$$

$$F_{y_{\text{des}}} = -\frac{(m \cos \psi \nu_2 + \sin \phi F_z - m \sin \psi \nu_1) \cos \phi}{\sin^2 \phi - 1}$$

$$\dot{\theta}_{\text{des}} = \frac{1}{V \cos \beta \cos \alpha \cos \phi} \left(-\sin \psi \sin \phi \nu_1 + \right. \\
+V \cos^2 \phi \cos \beta \cos \alpha q + \\
+\cos \theta \cos \phi \nu_3 + F_z/m + \\
-V \sin \phi \cos \phi \cos \beta \cos \alpha r + \\
+\sin \phi \cos \psi \nu_2 - \sin \theta \sin \psi \cos \phi \nu_2 + \\
\left. -\cos \psi \sin \theta \cos \phi \nu_1 \right)$$

References

- [1] S. N. Singh, P. Chandler, C. Schumacher, S. Banda, and M. Pachter, "Nonlinear adaptive close formation control of unmanned aerial vehicles," *Dynamics and Control*, vol. 10, no. 2, pp. 179–194, April 2000.
- [2] A. W. Bloy, M. G. West, K. A. Lea, and M. Jouma'a, "Lateral aerodynamic interference between tanker and receiver in air-to-air refuelling," *Journal of Aircraft*, vol. 30, pp. 705–710, 1993.
- [3] A. W. Bloy and M. Jouma'a, "Lateral and directional stability control in air-to-air refuelling," *Journal of Aerospace Engineering*, vol. 209, pp. 299–305, 1995.
- [4] M. Pachter, J. J. D'Azzo, and A. W. Proud, "Tight formation flight control," *Journal of Guidance, Control and Dynamics*, vol. 24, no. 2, pp. 246–254, March–April 2001.
- [5] Proud, A. W., Pachter, M., and D'Azzo, J. J., "Close formation flight control," in *AIAA Guidance, Navigation and Control Conference*. Portland, OR: AIAA Paper 99-4207, August 1999.
- [6] M. Pachter, J. J. D'Azzo, and J. Dargan, "Automatic formation flight control," *Journal of Guidance, Control and Dynamics*, vol. 17, no. 6, pp. 1380–1383, November–December 1994.
- [7] Buzogany, L. E., Pachter, M., and D'Azzo, J. J., "Automated control of aircraft in formation flight," in *AIAA Guidance, Navigation and Control Conference*, Monterey, CA, August 1993, pp. 1349–1370.
- [8] S. S. Stankovic, M. Stanojevic, and D. D. Siliak, "Decentralized overlapping control of a platoon of vehicles," *IEEE Transaction on Control Systems Technology*, vol. 8, no. 5, pp. 816–832, September 2000.
- [9] D. R. Gingras, "Experimental investigation of a multi-aircraft formation," in *AIAA Applied Aerodynamics Conference*. Norfolk, VA: AIAA Paper 99-3143, June 1999.
- [10] D. R. Gingras, J. L. Player, and W. B. Blake, "Static and dynamic wind tunnel testing of air vehicles in close proximity," in *AIAA Atmospheric Flight Mechanics Conference and Exhibit*. Montreal, Canada: AIAA Paper 2001-4137, August 2001.
- [11] R. C. Nelson and E. J. Jumper, "Aircraft wake vortices and their effect on following aircraft," in *AIAA Atmospheric Flight Mechanics Conference and Exhibit*. Montreal, Canada: AIAA Paper 2001-4073, August 2001.

- [12] M. R. Anderson and A. C. Robbins, "Formation flight as a cooperative game," in *AIAA Guidance, Navigation and Control Conference*. Philadelphia, PA: AIAA Paper 98-4124, August 1998.
- [13] F. Giulietti, L. Pollini, and M. Innocenti, "Autonomous formation flight," *IEEE Control Systems Magazine*, vol. 20, no. 6, pp. 34–44, December 2000.
- [14] B. L. Stevens and F. L. Lewis, *Aircraft Control and Simulation*. New York: John Wiley & Sons, 1992.
- [15] J. J. Slotine and W. Li, *Applied Nonlinear Control*. Prentice-Hall, 1991, ch. 6, pp. 265–270.
- [16] G. Campa, M.R. Napolitano, *et al.*, "Design of control laws for maneuvered formation flight," *American Control Conference.*, vol. 3, pp. 2344 – 2349, 30 June-2 July 2004.